

# Exact Analysis of Three-Phase Rectifiers With Constant Voltage Loads

Predrag Pejović and Johann W. Kolar

**Abstract**—In this paper, an exact solution of a circuit model for a three-phase rectifier with constant-voltage load and ac-side reactance that operates in the continuous conduction mode is presented. Obtained results are compared to the results provided applying sinusoidal approximation, published previously. It is shown that the sinusoidal approximation provides acceptable results at low output voltages, with the accuracy being decreased for the output voltages approaching to the discontinuous conduction mode boundary. Computational complexity of the exact solution is about the same as for the solution obtained applying sinusoidal approximation.

**Index Terms**—Alternator, commutation, converter, generator, load matching, load regulation.

## I. INTRODUCTION

THE TOPIC of this paper is an exact solution for the electric circuit model of the rectifier presented in Fig. 1 for the continuous conduction operating mode. The rectifier of Fig. 1 is assumed to provide constant output voltage  $V_{OUT}$ , thus the load and the output filter are represented by a constant voltage source. It is also assumed that the rectifier is supplied by a three-phase voltage source by symmetrical ac side reactance, having an inductance  $L$  per phase. Although it might be expected that analysis of such circuit is readily available in literature, according to a detailed search presented in [1] it was not the case. Thus, in [1] analysis of the circuit presented in Fig. 1 is approached applying sinusoidal approximation [2].

Other relevant previous results include analyses of single-phase rectifiers with ac-side impedance and capacitive loading [3]–[7]. Three-phase rectifiers are treated in [8]–[11]. These analyses primarily focus to inductive or constant-current loads, with some exemptions. In [8], rectifiers with ac-side reactance and capacitive loading are analyzed, but covered topologies are single-phase and three-phase midpoint rectifiers. In [10], normalized diagrams obtained applying simulation methods are presented for three-phase rectifiers with capacitive loading and ac-side reactance, but they cover discontinuous conduction mode. In [11], the rectifier model the

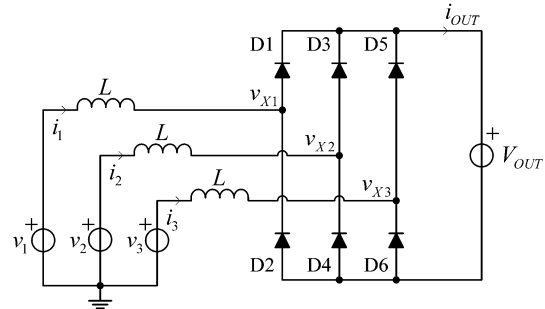


Fig. 1. Three-phase diode bridge rectifier with a constant-voltage load and ac-side reactance.

same as presented in Fig. 1 is briefly analyzed applying simulation methods, but the analysis is restricted to the discontinuous conduction mode at high output voltages.

In this paper, analytical expressions for the rectifier input currents will be derived, which is a basis to derive other analytical expressions, like the dependence of the output voltage on the output current, etc. Results of the exact analysis of the rectifier model will be compared to the results obtained applying sinusoidal approximation.

## II. ANALYSIS OF THREE-PHASE DIODE RECTIFIER WITH CONSTANT VOLTAGE LOAD

Let us assume that the rectifier of Fig. 1 is supplied by a balanced undistorted three-phase voltage system

$$v_k = V_m \sin\left(\omega t - (k-1)\frac{2\pi}{3}\right) \quad (1)$$

for  $k \in \{1, 2, 3\}$ . In order to generalize the results, let us normalize all voltages using the phase voltage amplitude as a base voltage

$$m = \frac{v}{V_m}. \quad (2)$$

According to this normalization, the output voltage is normalized to

$$M_{OUT} = \frac{V_{OUT}}{V_m}. \quad (3)$$

The analysis presented here is based on representation of the rectifier diodes by ideal diode models. However, in the case the diodes should be represented taking forward voltage drop into account, the output voltage in that case could readily be

Manuscript received September 3, 2007; revised December 29, 2007. First published July 18, 2008; last published August 13, 2008 (projected). This paper was recommended by Associate Editor B. C. Lesieutre.

P. Pejović is with the University of Belgrade, School of Electrical Engineering, 11120 Belgrade, Serbia (e-mail: peja@etf.bg.ac.yu).

J. W. Kolar is with Power Electronic Systems Laboratory, Swiss Federal Institute of Technology Zurich, ETH-Zentrum/ETL, CH-8092 Zurich, Switzerland (e-mail: kolar@lem.ee.ethz.ch).

Digital Object Identifier 10.1109/TCSII.2008.922462

obtained subtracting twice the forward voltage drop from the output voltage obtained in the case the diodes are ideal. In terms of the notation applied in [1], this means

$$V_{\text{OUT}} = V_o + 2V_d. \quad (4)$$

To simplify the notation further, let us normalize all of the rectifier currents taking  $V_m/\omega L$  as a base current

$$j = \frac{\omega L}{V_m} i \quad (5)$$

and let us represent the time variable by a phase angle equivalent

$$\varphi = \omega t. \quad (6)$$

After the normalization is introduced, the inductor equations in the circuit of Fig. 1

$$L \frac{di_k}{dt} = v_k - v_{Xk} \quad (7)$$

for  $k \in \{1, 2, 3\}$  are transformed to

$$\frac{dj_k}{d\varphi} = m_k - m_{Xk}. \quad (8)$$

In the analysis that follows, symmetries of the voltages and currents at the rectifier ac side, summarized by

$$j_1(\varphi) = j_2\left(\varphi + \frac{2\pi}{3}\right) = j_3\left(\varphi + \frac{4\pi}{3}\right) \quad (9)$$

and

$$m_{X1}(\varphi) = m_{X2}\left(\varphi + \frac{2\pi}{3}\right) = m_{X3}\left(\varphi + \frac{4\pi}{3}\right) \quad (10)$$

are going to be used frequently. Besides of this type of symmetry, the circuit of Fig. 1 also exposes a half-period symmetry given by

$$j_k(\varphi) = -j_k(\varphi + \pi) \quad (11)$$

and

$$m_{Xk}(\varphi) = -m_{Xk}(\varphi + \pi) \quad (12)$$

for  $k \in \{1, 2, 3\}$ .

According to [1], voltages at the diode bridge input terminals are given by

$$m_{Xk} = \frac{M_{\text{OUT}}}{2} \times \left( \text{sgn}(j_k) - \frac{1}{3}(\text{sgn}(j_1) + \text{sgn}(j_2) + \text{sgn}(j_3)) \right). \quad (13)$$

Applying symmetry properties (9) and (11) to determine signs of the rectifier input currents, and defining  $\phi$  as the first rising zero crossing of  $j_1(\varphi)$  for  $\varphi > 0$ , the waveform of  $m_{X1}$  is for  $M_{\text{OUT}} = 1.2$  obtained as depicted in the second diagram of Fig. 2. The waveforms of  $m_{X1}$ ,  $m_{X2}$ , and  $m_{X3}$  are obtained as piecewise constant, taking constant values over  $\pi/3$  phase angle segments. According to (13), there are four distinct values these voltages can take,  $\pm(1/3)M_{\text{OUT}}$  and  $\pm(2/3)M_{\text{OUT}}$ .

Applying the symmetry given by (11) and the fact that the inductor currents are continuous in time, we have

$$j_1(\phi + \pi) = j_1(\phi) = 0. \quad (14)$$

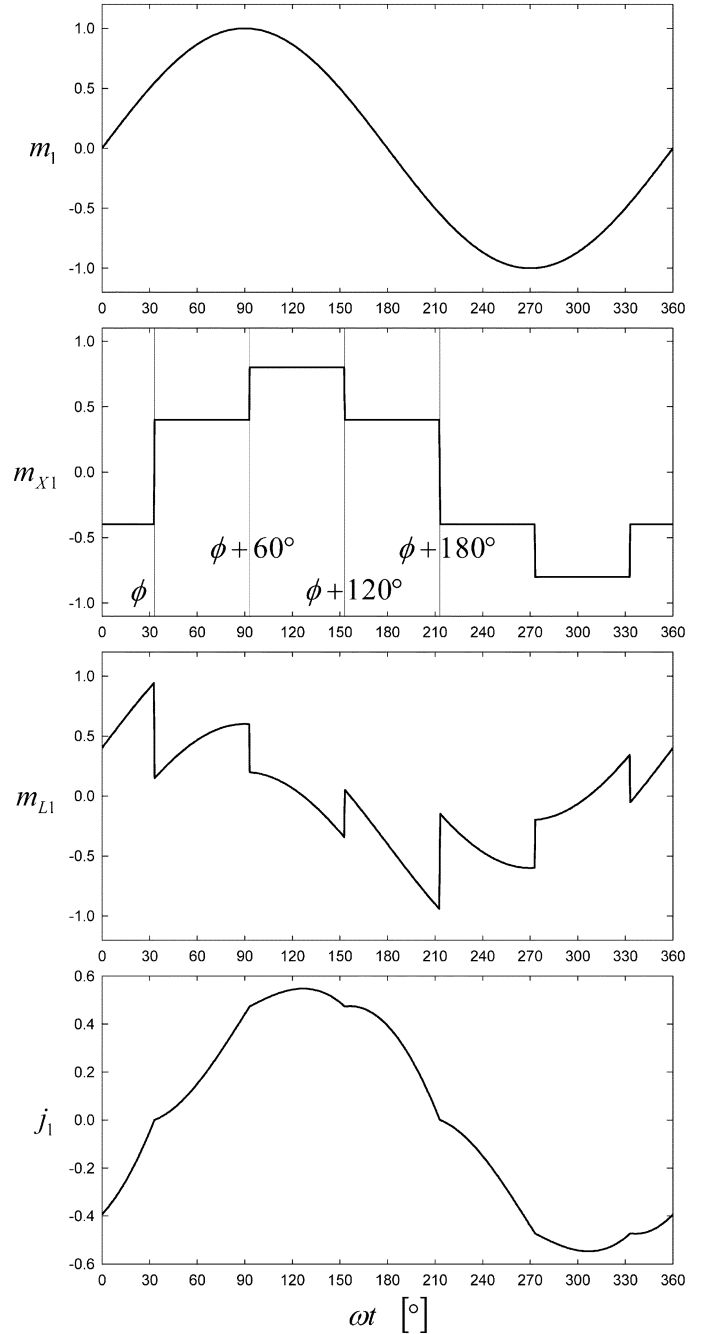


Fig. 2. Waveforms at the ac side of the first phase of the rectifier.

Integrating (8) and substituting in (14), taking the waveform of  $m_{X1}$  as depicted in Fig. 2, we obtain

$$\int_{\phi}^{\phi+\pi} (m_1(\varphi) - m_{X1}(\varphi)) d\varphi = 2 \cos \phi - \frac{4\pi}{9} M_{\text{OUT}} = 0 \quad (15)$$

which results in

$$\phi = \arccos\left(\frac{2\pi}{9} M_{\text{OUT}}\right). \quad (16)$$

$$j_1(\varphi) = \begin{cases} \left( \frac{2\pi}{9} + \frac{1}{3}(\phi - \varphi) \right) M_{\text{OUT}} - \cos(\varphi), & \text{for } \phi < \varphi < \phi + \frac{\pi}{3} \\ \left( \frac{\pi}{3} + \frac{2}{3}(\phi - \varphi) \right) M_{\text{OUT}} - \cos(\varphi), & \text{for } \phi + \frac{\pi}{3} < \varphi < \phi + \frac{2\pi}{3} \\ \left( \frac{\pi}{9} + \frac{1}{3}(\phi - \varphi) \right) M_{\text{OUT}} - \cos(\varphi), & \text{for } \phi + \frac{2\pi}{3} < \varphi < \phi + \pi \end{cases} \quad (17)$$

This is the key moment in obtaining the exact solution. After the zero crossing angle  $\phi$  is obtained, waveform of the input current at the first phase is applying (8) obtained as (17), shown at the bottom of the page, for  $\phi < \varphi < \phi + \pi$ . For the remaining half period,  $j_1$  is computed applying (11), while the waveforms of the remaining two of the phase currents are determined by (9). Waveform of the inductor voltage  $m_{L1} = m_1 - m_{X1}$  at the first phase is presented in the third diagram of Fig. 2, while the corresponding input current waveform is presented in the fourth diagram of the same figure.

The output current of the rectifier is computed as a dc component of the current flowing through the dc voltage source that models the load,

$$J_{\text{OUT}} = \frac{1}{2\pi} \int_0^{2\pi} (j_{D1}(\varphi) + j_{D2}(\varphi) + j_{D3}(\varphi)) d\varphi. \quad (18)$$

Applying symmetry and the knowledge about the input current signs during the period, (18) could be reduced to a computationally simpler form

$$J_{\text{OUT}} = \frac{3}{2\pi} \int_{\phi}^{\phi+\pi} j_1(\varphi) d\varphi \quad (19)$$

which provides the analytical expression that relates the output voltage and the output current

$$J_{\text{OUT}} = \frac{1}{3\pi} \sqrt{81 - 4\pi^2 M_{\text{OUT}}^2}. \quad (20)$$

Normalized value of the rectifier output power is

$$P_{\text{OUT}} = M_{\text{OUT}} J_{\text{OUT}} = \frac{M_{\text{OUT}}}{3\pi} \sqrt{81 - 4\pi^2 M_{\text{OUT}}^2} \quad (21)$$

and it reaches maximum of

$$P_{\text{OUT MAX}} = \frac{27}{4\pi^2} \approx 0.6839 \text{ p.u.} \quad (22)$$

at the output voltage

$$M_{\text{OUT}} = \frac{9\sqrt{2}}{4\pi} \approx 1.0128 \quad (23)$$

which is within the limits of the continuous conduction mode.

In the same manner, RMS value of the input currents is computed as

$$J_{\text{RMS}} = \frac{\sqrt{6}}{54} \sqrt{2M_{\text{OUT}}^2(5\pi^2 - 108) + 243} \quad (24)$$

and the power factor observed by the ideal voltage sources is obtained as

$$\text{PF} = \frac{2}{\pi} M_{\text{OUT}} \sqrt{\frac{243 - 12\pi^2 M_{\text{OUT}}^2}{243 - (216 - 10\pi^2) M_{\text{OUT}}^2}}. \quad (25)$$

All of the results are derived for the converter operating in the continuous conduction mode. Analyzing the waveforms, the critical point for the continuous conduction mode is the state transition at  $\phi$ , where the input current should continue to grow after the inductor voltage is reduced by the circuit commutation. The condition could be expressed as

$$\sin(\phi) > \frac{1}{3} M_{\text{OUT}} \quad (26)$$

that can be transformed applying the phase angle (16) to

$$M_{\text{OUT}} < \frac{9}{\sqrt{9 + 4\pi^2}} \approx 1.2926. \quad (27)$$

The continuous conduction mode boundary is derived in [1] applying the same condition as given by (26), but due to the difference in the phase angle [1, eq. (24)] the limit given by of [1, eq. (34)] is somewhat higher

$$M_{\text{OUT SA}} < \frac{3\pi}{\sqrt{36 + \pi^2}} \approx 1.3916. \quad (28)$$

### III. COMPARISON OF RESULTS

After the exact solution is obtained, it is interesting to compare the results to the results obtained applying sinusoidal approximation. The result for the phase angle of the first rising zero crossing of the first phase current is in [1] given by (24), which is in the notation applied in this paper

$$\phi_{\text{SA}} = \arctan \left( \sqrt{\left( \frac{\pi}{2M_{\text{OUT}}} \right)^2 - 1} \right). \quad (29)$$

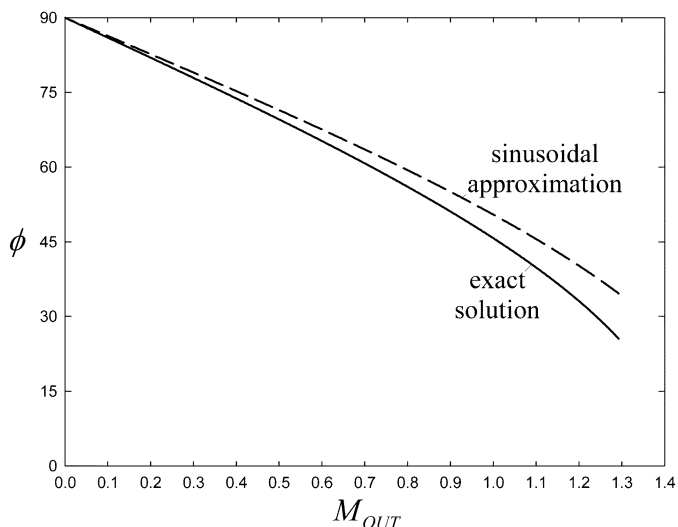


Fig. 3. Comparison of results for the phase displacement.

The curve determined by (29) is plotted in Fig. 3 by the dashed line, while the solid line presents the exact solution given by (16). It should be mentioned here that (29) has a physical meaning of the phase displacement between the phase voltage and the phase current in [1], while (16) does not have that meaning since the input currents analyzed in this paper contain higher order harmonics. However, in both of the cases  $\phi$  represents phase lagging of the waveform of  $v_{Xk}$  in comparison to the corresponding phase voltage  $v_k$  for  $k \in \{1, 2, 3\}$ .

Probably the most interesting of the comparisons is the comparison of the output current equations. Reference [1, eq. (25)] is in the notation applied in this paper expressed as

$$J_{OUT,SA} = \frac{3}{\pi} \sqrt{1 - \left(\frac{2}{\pi} M_{OUT}\right)^2}. \quad (30)$$

This curve is in Fig. 4 plotted by the dashed line, while (20) is plotted by the solid line. In the diagram of Fig. 4 it can be observed that agreement between the curves is good at low output voltages, where the input currents are slightly distorted. However, the difference grows as the output voltage grows, reaching the maximum at the continuous conduction mode boundary where the sinusoidal approximation predicts 31.87% higher output current than the exact solution.

The result for the power factor obtained applying sinusoidal approximation, given by [1, eq. (26)], is expressed in the notation applied in this paper as

$$PF_{SA} = \frac{2}{\pi} M_{OUT} \quad (31)$$

and differs from the exact expression for the power factor given by (25) only in the correction factor under the square root of (25). Agreement of the results is excellent, since the sinusoidal approximation provides the result that is about 0.11% higher than the exact value, with the relative error almost independent on the output voltage.

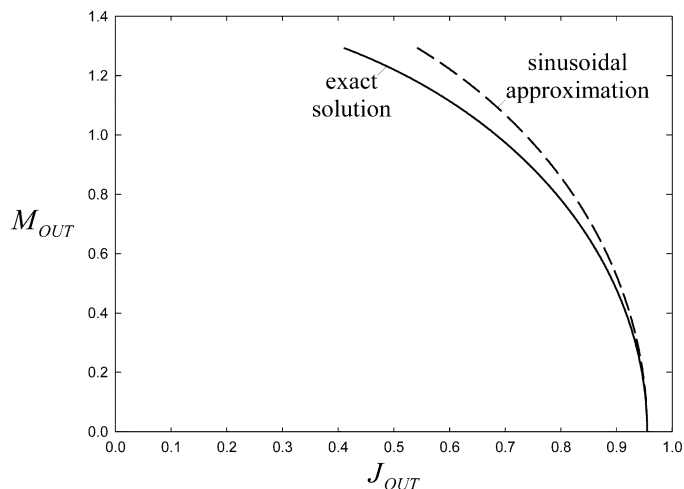


Fig. 4. Comparison of results for the output current.

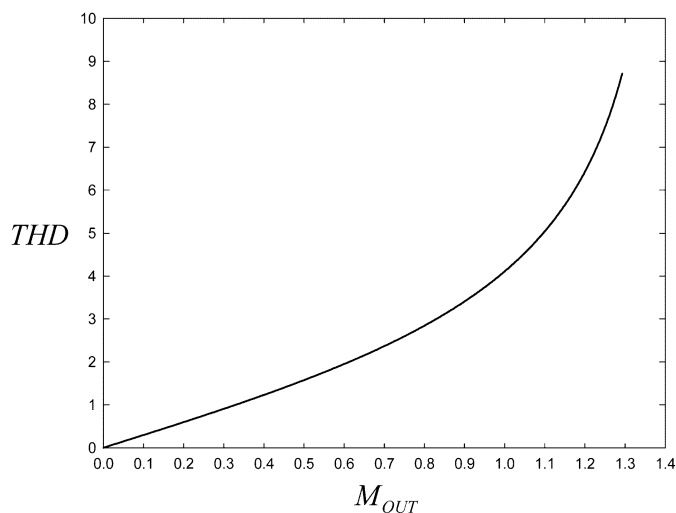


Fig. 5. Dependence of the input current THD on the output voltage.

The basic idea that stands behind the sinusoidal approximation is to neglect the higher order harmonics. Thus, THD of the input currents cannot be computed applying the sinusoidal approximation. Dependence of the input current THD on the output voltage obtained by the exact analysis is plotted in Fig. 5. As expected, the THD is low for low output voltages, reaching the maximum of about 9% at the continuous conduction mode boundary.

General conclusion from the comparisons is that the input currents are slightly distorted in the continuous conduction mode and that sinusoidal approximation is appropriate, providing somewhat inaccurate results only in predicting the output currents close to the continuous conduction mode boundary. However, the exact solution of the rectifier model has about the same computational complexity, but provides the exact result. On the other hand, cases when the supplying reactance contains a resistive component are not covered by the exact solution, and sinusoidal approximation is an option to get some results. In the case higher accuracy of the results is required, numerical simulation of normalized circuit model should be applied.

## IV. CONCLUSION

Exact solution of the rectifier model for a three-phase diode bridge rectifier loaded by a constant voltage load and supplied from symmetrical voltage sources by ac-side inductance is presented in this paper. Normalization of the rectifier voltages and currents is proposed in order to simplify the analysis and to generalize the results. Waveforms of the input currents are derived, as well as the dependence of the output voltage on the output current. Maximum of the dc power that can be supplied to the load is derived, as well as the input current RMS value and the power factor. Exact limit for the rectifier output voltage to provide operation in the continuous conduction mode is derived. Obtained results are compared to the results provided applying sinusoidal approximation. It is shown that sinusoidal approximation provides generally acceptable results, being more accurate at lower output voltages, where harmonic distortions of the input currents are lower. At the continuous conduction mode boundary, the sinusoidal approximation predicts 31.87% higher output current than the exact solution, which is the highest discrepancy between the solutions. Besides the results obtained applying sinusoidal approximation, the exact solution of the rectifier model provides information about the input current THD. Both of the solutions have about the same computational complexity.

## REFERENCES

- [1] V. Caliskan, D. J. Perreault, T. M. Jahns, and J. G. Kassakian, "Analysis of three-phase rectifiers with constant-voltage loads," *IEEE Trans. Circuits Syst. I, Fundam. Theory Appl.*, vol. 50, no. 9, pp. 1220–1226, Sep. 2003.
- [2] R. W. Erickson and D. Maksimović, *Fundamentals of Power Electronics*, 2nd ed. Norwell, MA: Kluwer Academic, 2001, pp. 709–740.
- [3] O. H. Schade, "Analysis of rectifier operation," *Proc. IRE*, vol. 31, pp. 341–361, 1943.
- [4] P. Richman, "Wave factors for rectifiers with capacitor input filters, and other high crest factor loads," *IEEE Trans. Ind. Electron. Contr. Instrum.*, vol. IECI-21, no. 11, pp. 235–241, Nov. 1974.
- [5] A. G. Bogle, "Rectifier circuit performance: Some new approximate formulas," *Proc. Inst. Elect. Eng.*, vol. 124, pp. 1127–1134, 1977.
- [6] W. P. Gibbons, "Current and voltage waveform distortion analysis on three-phase "wye" power systems with rectifier loads," *IEEE Trans. Ind. Appl.*, vol. IA-19, no. 2, pp. 181–190, Mar./Apr. 1983.
- [7] K. S. Hall, "Calculation of rectifier-circuit performance," in *Proc. Inst. Elect. Eng. A*, 1980, vol. 127, pp. 54–60.
- [8] J. Schaefer, *Rectifier Circuits: Theory and Design*. New York: Wiley, 1965.
- [9] A. W. Kelley and W. F. Yadusky, "Rectifier design for minimum line-current harmonics and maximum power factor," *IEEE Trans. Power Electron.*, vol. 7, no. 4, pp. 332–341, Apr. 1992.
- [10] M. Grotzbach and R. Redmann, "Line current harmonics of VSI-fed adjustable-speed drives," *IEEE Trans. Ind. Appl.*, vol. 36, no. 2, pp. 683–690, Mar./Apr. 2000.
- [11] N. Mohan, T. M. Undeland, and W. P. Robbins, *Power Electronics—Converters, Applications, and Design*, 3rd ed. Hoboken, NJ: Wiley, 2003, pp. 109–111.